Brittle rock fracture and progressive damage in potash

D. Stead[a], E. Eberhardt[b] and Z.Szczepanik[c]

[a]Camborne School of Mines, University of Exeter, Redruth, Cornwall, UK, TR15 3SE

[b]Engineering Geology, Swiss Federal Institute of Technology (ETH), Zurich, Switzerland.

[c]Department of Geological Sciences, University of Saskatchewan, Saskatoon, Canada. S7N 0W0

This paper examines the importance of brittle rock fracture and progressive damage in potash. Results of laboratory testing using integrated stress-strain-acoustic measurements are presented for both conventional uniaxial compression testing and creep. Changes in acoustic emission and acoustic velocity are used to characterise progressive damage during uniaxial loading. The relevance of the laboratory data to near-field rock behavior in potash mines is reviewed.

1. INTRODUCTION

The importance of brittle rock fracture and progressive damage around potash mine openings has been well documented. This near-field damage zone has been variously described as the disturbed rock zone (DRZ) or the excavation damage zone (EDZ). This paper presents typical results from a 10 year research program on Saskatchewan potash to illustrate how integrated acoustic strain measurements can be used to further our understanding of damage at uniaxial stresses. Stead et al. (1998) illustrated the use of both in-situ active and passive acoustic techniques in investigating damage around underground potash mine openings. Holcomb (1999) describes the use of 270 cross-borehole ultrasonic measurement paths in successfully characterising time-dependent damage around an air intake shaft at the Waste Isolation Plant, New Mexico. The potential use of acoustic techniques in the development of damage based constitutive criteria for saltrocks has been also been demonstrated by Chan et al. (1995), Munson et al. (1995), and Matei and Critescu (1999). Numerous factors influence the nature and origin of damage around potash openings including the stress path history, (mining method), time, mineralogy, grain size and texture, and environment (humidity and temperature). In laboratory characterisation of potash damage, further complications arise due to sampling effects, loading geometry and scale. Li et al. (1999) emphasise the importance of time and scale effects in the derivation of failure criterion.

2. CRACK INITIATION AND DAMAGE THRESHOLDS IN POTASH

2.1 Experimental Technique

A series of uniaxial compression tests were performed on samples of potash from a Saskatchewan mine. Grain sizes in the samples varied from a minimum of 4 mm to a maximum of 40 mm, with an average grain size between 10 and 15 mm. Clay content was minor and dispersed. Cylindrical samples were prepared for testing according to ASTM standards with lengths of 230 mm and diameters of 110 mm. Prior to uniaxial testing, P- and S-wave travel times were recorded for all samples with a mean of 3950m/s and 2520m/s respectively. Samples were then loaded at an average rate of 4 MPa/minute. Each sample was instrumented

with four 51 mm (2 inch) electric resistance strain gauges (2 axial and 2 lateral at 90° intervals) to record sample deformation. Strain gauge measurements were made using a sampling rate of 2 readings per second to allow indications of crack initiation/growth from axial and lateral stress-strain curves. A moving point regression technique, which uses the first derivative of the stress-strain curves to highlight any slope or rate changes, was used in the investigation of crack closure/initiation and damage stresses, Eberhardt et al. (1998). In addition to the use of strain gauges, the acoustic emission (AE) response was also recorded using two 175 kHz resonant frequency piezoelectric transducers. Transducers were mounted using wave-guides epoxied to the sample surface and provided a solid coupling. The monitoring system consisted of a bandpass filter with a frequency range of 125 kHz to 1 MHz and a pre-amplifier with 40dB total gain. The AE data was recorded with an AET 5500 acoustic emission monitoring system using a threshold value of 0.1 V. AE properties including ring-down count, peak amplitude, event duration and rise time were used in the analysis.

2.2. Analysis of Uniaxial Data

It is generally accepted that the first fractures in a uniaxially loaded sample are tensile microcracks (Lajtai and Lajtai, 1974). The propagation of these cracks has been shown to occur in the direction of the major principal stress (σ_1), where cracks not aligned with σ_1 grow along a curved path to align themselves with σ_1. The opening of crack faces parallel to the applied load and the closure of crack faces perpendicular to the load cause certain changes in the relative lateral and axial deformations, respectively. Stiffness plots were created from the test data using the moving point regression analysis to highlight any changes in strain rate which, in turn, may be used to identify different stages of rock deformation and crack development leading up to failure. Examination of the stiffness plots reveals that the potash displays its stiffest and most elastic behaviour during the initial stages of loading (the axial stiffness is equivalent to a moving average of the deformation modulus). A typical axial stiffness plot is shown in Figure 1. The potash exhibits its most linear behaviour from the commencement of loading, at between 3MPa and 6 MPa (or between 0.1 and 0.25 σ_{UCS}).

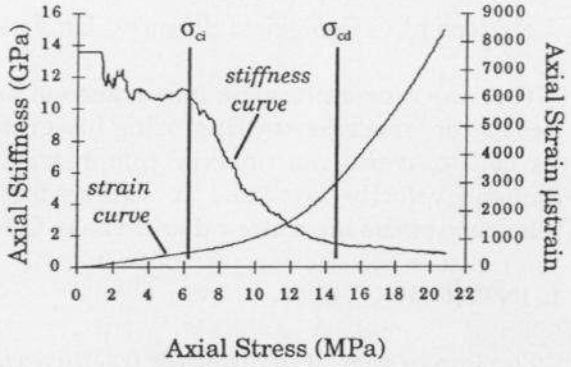

Figure 1. Axial strain –v strain data showing changes in axial stiffness during uniaxial loading.

A significant number of the pre-existing cracks may have closed during the first 2 MPa of loading before the sample, loading platen and strain gauges could become fully coupled. It is likely that some crack closure, as well as intracrystalline plastic strain, occurred during the initial stages of loading but not at significant enough levels to influence the measured strain. Examination of the acoustic emission response (Fig. 2) indicates that the onset of significant cracking begins at approximately 25% of the uniaxial compressive strength of the potash. This point is interpreted as being the crack initiation threshold (σ_{ci}). AE activity prior to this point can be attributed to movement along crack faces or minor cracking along planes previously weakened through the

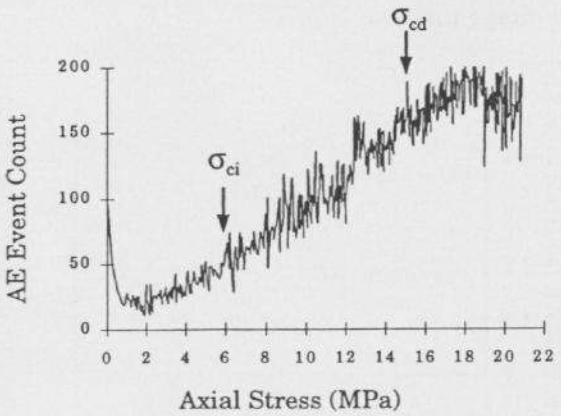

Figure 2. AE event count vs. axial stress during uniaxial loading of potash.

sampling process. Examination of Figure 1 indicates that once cracking is initiated, the propagation of these cracks results in a continuous reduction in sample stiffness. In addition, decreases in both the axial and lateral stiffness values indicate that tensile microfracturing is not the only mechanism responsible for the increase in deformation. Theoretically, induced tensile cracking should only influence the lateral strain rate. It has been well established that crack propagation occurs in the σ_1 direction (i.e. the axial direction), therefore the opening of these cracks should be detected perpendicular to this motion in the lateral direction. The opening of these tensile cracks can be clearly seen on the surface of tested specimens. Significant reductions in the axial stiffness following the σ_{ci} threshold may indicate that deformation of large potash crystals, in association with tensile microfracturing. A similar explanation was given by Lajtai *et al.*(1994) to explain the same phenomenon. Crack coalescence may also contribute to unexpected axial deformations. As cracks increase, both in number and size, they will eventually begin to interact with one another. Crack interaction then becomes extremely complex as stress shadows overlap. Stable crack propagation continues until the onset of dilatancy that, in turn, marks the beginning of unstable crack growth. The determination of this threshold, referred to hereafter as the crack damage stress threshold (σ_{cd}), is relatively straight forward as it is marked by the reversal of the volumetric strain curve. This point stands out very clearly in the derivative volumetric stiffness plot where the slope changes from positive to negative at approximately 0.5 σ_{UCS} (Fig.3). The crack damage threshold marks a point where the AE event count reaches a relatively constant level. Figure 3 reveals that throughout stable crack propagation, the number of detected events continuously increases. Once unstable crack propagation begins (i.e. σ_{cd}), the number of events peak and remain constant until failure. It was observed that although the number of events

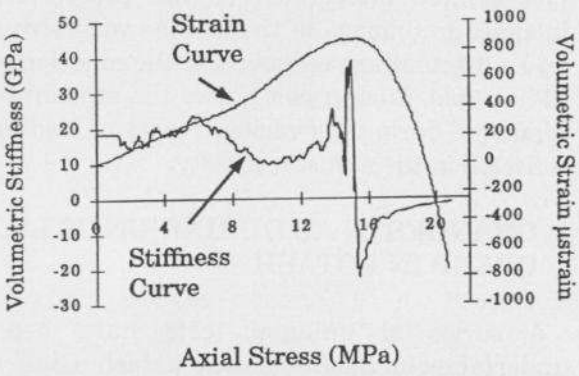

Figure 3. Volumetric stiffness vs. axial stress during uniaxial loading of potash.

remains constant, the ringdown counts and rise times of the events themselves continue to increase. Smaller increases in the other event properties (i.e. event duration and peak amplitude) are also observed after the σ_{cd} threshold. This would seem to indicate that larger AE events are accompanying unstable crack propagation. These larger events may also indicate the occurrence of different deformation and

fracture mechanisms. Figure 1 indicates that the stiffness of the potash reaches a relatively constant but significantly reduced level at the σ_{cd} threshold. The large strains observed from this point until failure are possibly due to a combination of plastic yield as well as the movement/buckling of columnar pieces of intact material bounded by large cracks.

Observations of the failed samples seems to indicate that the final mode of failure was linked to a complex combination of shear and buckling of columnar pieces shaped by large cracks parallel to the loading direction. These large cracks which extend from one end of the sample to the other are analogous to the large vertical tensile fractures, several meters in length, commonly observed in potash mines, (Lajtai *et al.*, 1994). Figure 4 shows a plot of the normalised AE with respect to the total numbers of acoustic events at failure. This plot can be interpreted as the progressive increase in damage of the sample with stress and a concomitant reduction in the cohesion of the sample. Such a plot shows the amount of "damage" during the various stages of loading reflected in the acoustic activity.

3. CHANGES IN AE DURING UNIAXIAL CREEP IN POTASH

A series of uniaxial tests have been undertaken on Saskatchewan potash using combined axial stress – acoustic emission measurements. The details of the experimental setup are described in Stead et al. (1998). Acoustic emission was found to be strain rate dependent and to occur in association with the well defined primary, secondary and tertiary creep stages. The progressive acoustic emission/axial strain may reflect the cumulative damage increase within the sample. A characteristic U-shaped acoustic emission event count-time curve has been reported, Stead and Szczepanik (1991). This may be re-interpreted in terms of normalised acoustic emission event count/minute vs. normalised axial strain to show that the nature of the damage process.

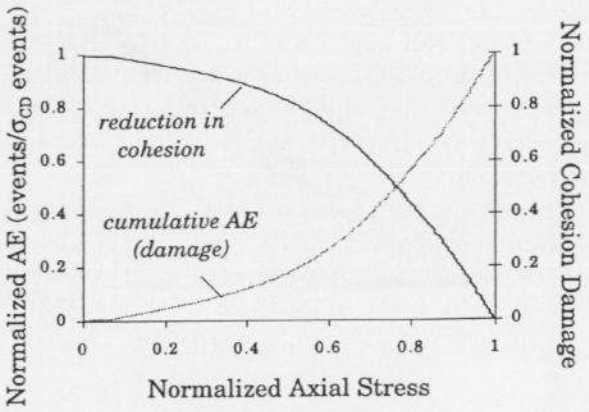

Figure 4. Progressive damage during uniaxial loading of potash.

Normalization is with respect to the total acoustic emission count and axial strain at failure. Figure 5 shows a plot of normalized acoustic events against normalized axial strain for a uniaxial creep test with a constant stress of 20MPa. Typically there are significant amounts of damage incurred during the initial loading and primary creep. This is reflected by high strain rates and acoustic emission counts.

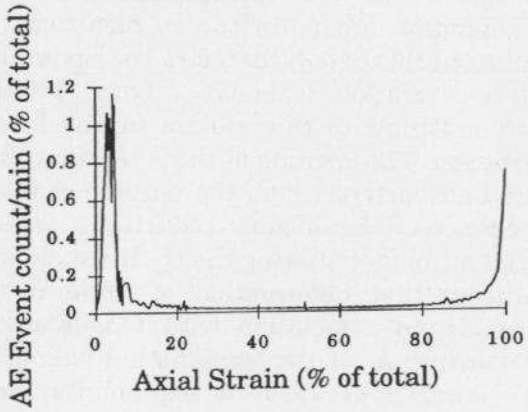

Figure 5. Normalised AE event count vs. axial strain for uniaxial creep test on potash.

Figure 6 is a plot of normalised cumulative acoustic emission vs. normalised cumulative axial strain and clearly shows the initial

high rate of acoustic emission associated with initial loading and primary creep. Examination of the results for the program of testing indicates that the shapes of these normalized plots of acoustic emission against strain may be useful indicators both of progressive damage and sample damage associated with pre-existing stresses or sampling. An increasing width in the initial peak in Figure 5 reflects high initial strain rates, which may be associated with closure

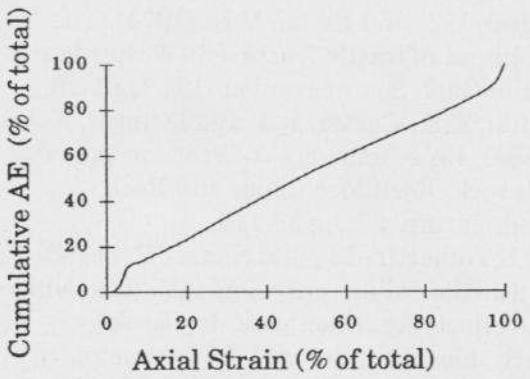

Figure 6. Normalized acoustic emission vs. axial strain plot for test shown in Fig.5

/propagation of pre-existing microcracks. The primary creep stage is followed by a low rate of acoustic emission activity with a linear increase in damage during the secondary creep stage. It should be emphasized that although the level of acoustic activity appears low, the largest amount of cumulative acoustic emission occurs during the secondary creep stage reflecting an increase in damage due to microcracking. Discrete high amplitude events are often observed within the generally low amplitude acoustic emission background. Tertiary creep is accompanied by a significant increase in the rate of acoustic emission activity with both larger and more frequent events as the damage accumulates until microfractures coalesce and sample failure occurs.

4. CHANGES IN ACOUSTIC VELOCITY DURING UNIAXIAL CREEP.

A series of uniaxial creep tests were conducted in which both P and S wave velocity determinations were made throughout. Examination of the data showed that the reduction in P and S wave velocity was closely related to the creep stages. Samples showed minor increases in velocity during the initial loading that may reflect healing of pre-existing damage. This was followed by reductions in velocity with time similar in trend to a typical uniaxial creep curve. The data was further analysed and showed clear changes in the both the amplitude of P- and S-Wave arrivals and the amplitude of the central frequency of the P and S-wave frequency spectra with time, Stead and Lu (1992). Figure 7 shows the relationship of the changes in the S-wave amplitude with time. It clearly demonstrates that the amplitude reduction may be a function of progressive increase in damage during creep.

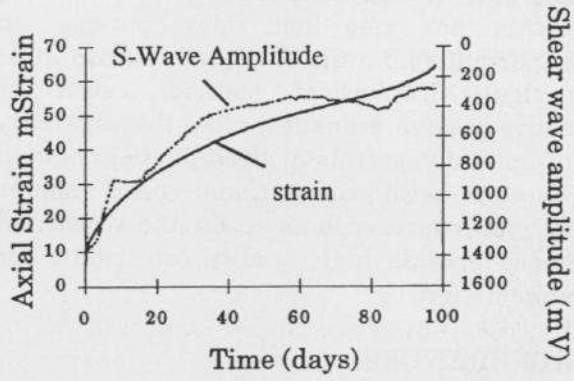

Figure 7. Changes in S-wave amplitude during uniaxial creep test on potash.

In addition to the progressive increase in damage the velocity data frequently indicated possible formation of macrocracks within the specimen as sharp changes in acoustic transmission behavior.

The correlation of near-field changes in acoustic emission, acoustic velocity and strain with progressive stress-induced damage is a promising area for future research.

5. CONCLUSIONS

The failure of near-field rock in potash mines involves mechanisms of progressive damage often at low confining stress conditions. In-situ studies have clearly shown the existence of well-defined damage zones within potash mine pillars that may lead to slabbing failure in the immediate wall, (Stead et al. 1998). This paper attempts to demonstrate the potential use of active-passive acoustic techniques, integrated with stress/strain measurement, in the laboratory characterization of stress-induced damage mechanisms in potash. Realistic numerical modeling of potash mine openings requires a further understanding of the near-field stress induced damage process around mine openings. It is suggested that an integrated approach involving both rock damage characterization and numerical modeling within the near-field may provide an important constraint for future potash mine design. Geophysical methods, such as active/passive acoustics, offer the capability to spatially correlate strength degradation /damage with conventional point source measurements such as strain and stress and hence provide high quality constraints for mine design.

REFERENCES

Chan, K.S., Bodner, S.R., Fossum, A.F. and Munson,D.E.(1995).Constitutive representation of damage healing in WIPP salt. Proc 35th U.S. Symp. Rock Mech. p485-490

Matei, A., and Critescu, N.D. (1999). Variation in time of the elastic parameters of rock salt. Proc. Int. Cong. On Rock Mech., p635-639, Paris.

Eberhardt, E., Stead, D., Stimpson, B. and Read, R.S. (1998). Identifying crack initiation and propagation thresholds in brittle rock. Can Geotech. Journ. 35:2 p222-233.

Holcomb, D.J. (1999). Assessing the Disturbed Rock Zone (DRZ) around a 655 meter vertical shaft in salt using ultrasonic waves. In "Rock mechanics for Industry". Eds. Amadei, Kranz, Scott and Smeallie, Proc US. Symp. Rock Mech., p965-972. Vail, Colorado.

Lajtai, E.Z. and Lajtai, V.N. (1974). The evolution of brittle fracture in rocks. Journ. of the Geol. Soc. of London. 130:1, p1-18.

Lajtai, E.Z., Carter, B.J. and Duncan, E.J.S. (1994). En echelon crack-arrays in potash salt rock. Rock Mechanics and Rock Engineering. 27:2, p89-111.

Li, L, Aubertin, M., and Simon, R. (1999) Multiaxial failure criterion with time and size effects for intact rock. In "Rock mechanics for Industry". Eds. Amadei, Kranz, Scott and Smeallie, Proc US. Symp. Rock Mech., p653-659,Vail, Colorado.

Munson, D.E., Holcomb, D.J., De Vries, K.L., Brodsky, N.S. and Chan, K.S. (1995). Correlations of theoretical calculations and experimental measurements of damage around salt. Proc. 35th U.S. Symp. Rock Mech., p491-496.

Stead, D. and Lu, C. (1992). Laboratory acoustic studies on rock types related to potash mining. Proc. CIM. A.G.M., Strata Control Session, p211-220, Montreal.

Stead, D., Szczepanik, Z., and Gaskin, W., (1998). Acoustic characterization of potash. p31-45. Proc. 4th Conference on the Mechanical Behavior of Salt, Ecole Polytechnique, Montreal.

Stead, D. and Szczepanik, Z. (1991). Time dependent acoustic emission studies on potash. Proc. 32nd U.S. Symp. Rock Mech., p471-479, Oklahoma.